

# Electrically conductive bacterial nanowires produced by *Shewanella oneidensis* strain MR-1 and other microorganisms

Yuri A. Gorby<sup>\*†</sup>, Svetlana Yanina<sup>\*</sup>, Jeffrey S. McLean<sup>\*</sup>, Kevin M. Rosso<sup>\*</sup>, Dianne Moyles<sup>‡</sup>, Alice Dohnalkova<sup>\*</sup>, Terry J. Beveridge<sup>‡</sup>, In Seop Chang<sup>§</sup>, Byung Hong Kim<sup>¶</sup>, Kyung Shik Kim<sup>¶</sup>, David E. Culley<sup>\*</sup>, Samantha B. Reed<sup>\*</sup>, Margaret F. Romine<sup>\*</sup>, Daad A. Saffarini<sup>||</sup>, Eric A. Hill<sup>\*</sup>, Liang Shi<sup>\*</sup>, Dwayne A. Elias<sup>\*\*\*</sup>, David W. Kennedy<sup>\*</sup>, Grigoriy Pinchuk<sup>\*</sup>, Kazuya Watanabe<sup>††</sup>, Shun'ichi Ishii<sup>††</sup>, Bruce Logan<sup>\*\*</sup>, Kenneth H. Nealson<sup>§§</sup>, and Jim K. Fredrickson<sup>\*</sup>

<sup>\*</sup>Pacific Northwest National Laboratory, Richland, WA 99352; <sup>‡</sup>Department of Molecular and Cellular Biology, University of Guelph, Guelph, ON, Canada N1G 2W1; <sup>¶</sup>Water Environment and Remediation Research Center, Korea Institute of Science and Technology, Seoul 136-791, Korea; <sup>§</sup>Department of Environmental Science and Engineering, Gwangju Institute of Science and Technology, Gwangju 500-712, Korea; <sup>||</sup>Department of Biological Sciences, University of Wisconsin, Milwaukee, WI 53211; <sup>\*\*</sup>Department of Agriculture Biochemistry, University of Missouri, Columbia, MO 65211; <sup>††</sup>Marine Biotechnology Institute, Heita, Kamaishi, Iwate 026-0001, Japan; <sup>\*\*</sup>Department of Environmental Engineering, Pennsylvania State University, University Park, PA 16802; and <sup>§§</sup>Department of Earth Sciences, University of Southern California, Los Angeles, CA 90089

Communicated by J. Woodland Hastings, Harvard University, Cambridge, MA, June 6, 2006 (received for review September 20, 2005)

***Shewanella oneidensis* MR-1 produced electrically conductive pilus-like appendages called bacterial nanowires in direct response to electron-acceptor limitation. Mutants deficient in genes for c-type decaheme cytochromes MtrC and OmcA, and those that lacked a functional Type II secretion pathway displayed nanowires that were poorly conductive. These mutants were also deficient in their ability to reduce hydrous ferric oxide and in their ability to generate current in a microbial fuel cell. Nanowires produced by the oxygenic phototrophic cyanobacterium *Synechocystis* PCC6803 and the thermophilic, fermentative bacterium *Pelotomaculum thermopropionicum* reveal that electrically conductive appendages are not exclusive to dissimilatory metal-reducing bacteria and may, in fact, represent a common bacterial strategy for efficient electron transfer and energy distribution.**

biofilms | cytochromes | electron transport | microbial fuel cells

Microbial dissimilatory reduction of metals is a globally important biogeochemical process driving the cycling of Fe, Mn, associated trace metals, and organic matter in soils and sediments as well as in freshwater and marine environments (1, 2). Most electron acceptors typically used by prokaryotes (oxygen, nitrate, sulfate, and carbon dioxide) are freely soluble both before and after reduction, whereas environmental Fe(III) and Mn(IV) exist predominantly as oxyhydroxide minerals. In anoxic environments, dissimilatory metal-reducing bacteria (DMRB) must overcome the fundamental problem of engagement of the cell's electron transport system (ETS) with poorly soluble minerals. DMRB have apparently developed several strategies, including (i) "shuttling" electrons by using humic acids (3) or cell metabolites (4) from terminal points of the ETS to the mineral surfaces, (ii) transferring electrons to Fe(III)- or Mn(IV)-bearing minerals directly via multiheme cytochromes associated with the outer membrane (5, 6), or (iii) through electrically conductive pili or "nanowires" (7). In this study, we provide evidence that the DMRB *Shewanella oneidensis* MR-1 produces electrically conductive nanowires in response to electron-acceptor limitation. We also show that electrically conductive nanowires are not restricted to metal-reducing bacteria, such as *Shewanella* and *Geobacter*, but are also produced by an oxygenic photosynthetic cyanobacterium and a thermophilic fermentative bacterium.

## Results

**Production of Extracellular Appendages Under O<sub>2</sub>-Limited Growth Conditions.** *S. oneidensis* MR-1 cells in continuous culture (chemostats) with electron-acceptor (O<sub>2</sub>) limitation and low agitation (50 rpm) consisted of aggregates with pilus-like appendages ranging

from 50 to >150 nm in diameter and extending tens of microns or longer (Fig. 1A; and see Fig. 5A, which is published as supporting information on the PNAS web site). Similar structures were observed by fluorescence microscopy when stained with a nonspecific fluorescent protein-binding stain (Fig. 1B). Similar structures were produced during anaerobic growth with either fumarate or Fe(III)-nitritotriacetic acid as dissolved electron acceptors, as long as the concentration of these electron acceptors were growth-limiting (data not shown). Few appendages were observed in chemostat cultures that were supplied with excess electron acceptor (O<sub>2</sub> > 2% of air saturation) but were otherwise identical to electron-acceptor-limited cultures (Fig. 5B).

Samples of cells with the extracellular appendages were collected from O<sub>2</sub>-limited cultures, applied to the surfaces of highly ordered pyrolytic graphite, and examined by scanning tunneling microscopy (STM) and tunneling spectroscopy to assess their ability to conduct an electrical current. STM images (constant-current topographs) of isolated appendages on the graphite surface revealed that their widths range from 50 to 150 nm (Fig. 2A). The apparent heights of the appendages in the STM images were ≈ 10 nm above the graphite surface (Fig. 2B), a value that was consistent with measurements obtained by scanning EM (SEM) and atomic force microscopy for these air-dried samples. For a conductive material, the apparent height should be close to the actual height of the sample, whereas, for a nonconductive sample, the apparent height should be 0. STM images also revealed that the appendages possessed a ridged structure running along their lengths (Fig. 2B). Ridges, typically with diameters of ≈ 3–5 nm, appeared as individual electrically conductive filaments, as revealed by STM images of "frayed" ends of appendages (Fig. 6, which is published as supporting information on the PNAS web site). Collectively, these results indicate that these appendages, which we have termed bacterial nanowires, are electrically conductive.

**Extracellular Reduction of Silica Ferrihydrite to Magnetite (Fe<sub>3</sub>O<sub>4</sub>) Nanoparticles by Bacterial Nanowires.** Given their ability to conduct electrons *in vitro*, we investigated the ability of nanowires to reduce and transform poorly crystalline silica ferrihydrite. *S. oneidensis*

Conflict of interest statement: No conflicts declared.

Freely available online through the PNAS open access option.

Abbreviations: DMRB, dissimilatory metal-reducing bacteria; HFO, hydrous ferric oxide; MFC, microbial fuel cell; STM, scanning tunneling microscopy.

<sup>†</sup>To whom correspondence should be addressed at: Biological Sciences Division, Pacific Northwest National Laboratory, P.O. Box 999, MS: P7-50, Richland, WA 99352. E-mail: yuri.gorby@pnl.gov.

© 2006 by The National Academy of Sciences of the USA



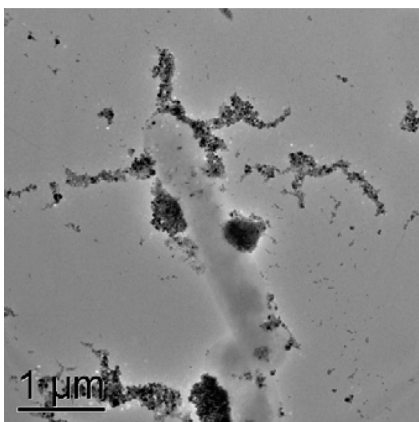


**Fig. 3.** Transmission EM images of whole mounts of MR-1 cells incubated in an aqueous suspension of Si-HFO. The Si-HFO was transformed to nanocrystalline magnetite along extracellular features consistent with the dimensions of nanowires.

MR-1 (Fig. 1). The apparent height of the GSPD appendages obtained by STM (Fig. 8C) was, however, almost two orders of magnitude less than for MR-1 (Fig. 2) with the same bias voltage and setpoint current. We were unable to obtain an STM image of the nanowires from  $\Delta$ MTRC/OMCA. These results indicate that the appendages produced by these mutants were poor electrical conductors relative to those produced by the wild-type MR-1.

Both  $\Delta$ MTRC/OMCA and GSPD mutants were impaired in their ability to reduce silica ferrihydrite (Table 1) and to produce electric current in a mediatorless microbial fuel cell (MFC) (Table 1). *S. oneidensis* MR-1 had been shown to have electrochemical activity in a mediatorless MFC (11), and this activity was attributed to the ability of MR-1 to localize cytochromes to the outer membrane where they facilitate the transfer of electrons to the electrode surface via a direct-contact mechanism. Interestingly, the extent of impairment of these mutants was similar for both the HFO reduction and electrochemical assays, providing further evidence that a similar extracellular electron-transfer mechanism is used for both processes.

**Production of Nanowires by Other Bacterial Genera.** Nanowire production is not exclusive to *S. oneidensis* strain MR-1. The photosynthetic cyanobacterium *Synechocystis* strain PCC 6803 produced electrically conductive nanowires when cultivated under conditions of CO<sub>2</sub> limitation (Fig. 4A). The structures were highly electrically conductive, as confirmed by STM and tunneling spectroscopy (Fig. 4B) and displayed a ridged appearance that was strikingly similar to bundled nanowires observed in *S. oneidensis* MR-1 (Fig. 2). Strain 6803 did not produce nanowires when CO<sub>2</sub> was provided in excess. Electrically conductive nanowires were also produced by a thermophilic fermentative bacterium *Pelotomaculum thermopropionicum*. SEM images revealed that *P. thermopropionicum* produced pilus-like filaments when it was grown in monocultures on fumarate

and in cocultures with *Methanothermobacter thermoautotrophicus* on propionate (Fig. 4C), as described (12). STM images and tunneling spectroscopy confirmed that these filaments were highly electrically conductive and were composed of bundles of individual electrically conductive filaments, each measuring between  $\approx$ 10 and 20 nm in diameter (Fig. 4D).

## Discussion

*S. oneidensis* MR-1 produces electrically conductive nanowires in response to O<sub>2</sub> limitation. In contrast to an earlier report (7), our STM results confirm that nanowires produced by MR-1 are efficient electrical conductors. STM imaging conditions were always stable, with no tendency for the tip to move the nanowires across the surface by intermittent contact unless conditions were specifically set to do so. We exclude the possibility that the current was being carried by ionic conduction from the possible presence of water and dissolved ions by examining the distance dependence of the tunneling current at various locations over appendages. These spectra consistently exhibited exponential current decay with increasing distance showing typical decay constants, a signature of true electron tunneling. In contrast, ionic conduction would have been identified by a linear current–distance relationship (13).

The discovery of bacterial nanowires and identification of the electron-transfer components that are required for electrical conductivity provide important advancements toward understanding the mechanisms involved in electron transfer from DMRB bacteria such as *Shewanella* and *Geobacter* to metal-oxide solids. Experience gained through our investigations underscores the need for extreme caution when designing experiments, making measurements, and interpreting results. Cultivation conditions, the fragile nature of nanowires, and the fact that most microorganisms can construct multiple pilus-like structures (14) can produce artifacts and, in the case of the report by Reguera *et al.* (7), likely led to the erroneous conclusion that extracellular appendages produced by strain MR-1 are not electrically conductive. We have observed that cells cultivated in nutrient-rich media or under high-agitation conditions that mechanically disrupt fragile extracellular appendages produce samples that contain abundant evidence of cellular debris and relatively few intact structures resembling nanowires (data not shown). Occasionally, pilus-like structures were observed that exhibited nonconductive behavior when investigated by STM and conduction atomic force microscopy. We conclude that such structures could represent products from a number of possible genes, including *mshA* (SO4104), *pilA* (SO0417), and, possibly, *gspG* (SO0169) of the type II secretion pathway.

Bacterial nanowires present important and logical implications for enzymatic reduction of solid phase iron and manganese oxides by DMRB, such as *Shewanella* and *Geobacter*. Nanowires may facilitate far-field transport of electrons from cells to solid phases located at significant distances from bacterial cells. These findings do not exclude the possibility that reduction of solid-phase iron oxides can occur by either direct cell-to-mineral contact or the use of dissolved low-molecular-mass compounds to shuttle electrons between bacteria and oxide minerals. However, multiple lines of evidence implicate nanowires as the major pathway for extracellular electron transfer in *S. oneidensis* MR-1, particularly in environments where cells are sessile. Direct visual evidence confirmed reductive transformation of poorly crystalline ferrihydrite into nanocrystalline magnetite along the length of bacterial nanowires. Additional research designed to critically and comprehensively evaluate far-field electron transfer via nanowires is needed to confirm these intriguing observations.

We have yet to conclusively identify the electrically conductive components of *Shewanella* nanowires. Our results demonstrate that MtrC and OmcA are required to produce electrically conductive nanowires and to transform hydrous ferric oxide into magnetite along extracellular structures that are morphologically identical to nanowires. Results correlating the loss of electrical conductivity, the

**Table 1. Metal-reduction and electrochemical properties of *S. oneidensis* MR-1, GSPD and  $\Delta$ MTRC/OMCA**

Strain	Ferrihydrite-reduction-extractable Fe(II),* mM	Electrochemical activity, mA
MR-1	2.17 $\pm$ 0.19	68.0 $\pm$ 7.8
$\Delta$ MTRC/OMCA	0.67 $\pm$ 0.13	14.3 $\pm$ 2.08
GSPD	0.42 $\pm$ 0.02	12.3 $\pm$ 0.58

\*HFO (20 mM) reduction sampled at 24 h and extracted with 0.5 N HCl overnight. Fe(II) was determined by using the ferrozine assay (30).



transduction and distribution via electrically conductive nanowires is both scientifically interesting and experimentally accessible. Further collaborative investigations into the complete composition of nanowires, mechanisms of electron flow through the wires, and interaction of nanowires between and among organisms in natural microbial communities are warranted to completely realize the implications of these structures in areas of alternative energy production, carbon sequestration, bioremediation, cell signaling, and, perhaps, pathogenicity and human health.

## Materials and Methods

**Bacterial Strains and Culture Conditions.** Cells of *S. oneidensis* strain MR-1 (wild-type), the double-deletion mutant  $\Delta$ MTRC/OMCA lacking two decaheme cytochromes, and the insertion mutant GSPD that does not produce outer membrane channel-forming proteins associated with the type II secretion system were cultured in continuous flow reactors (New Brunswick Scientific) operating in chemostat mode with a dilution rate of  $0.1 \cdot \text{h}^{-1}$  and an operating liquid volume of 3 liters. A chemically defined medium contained the following: sodium lactate, 18 mmol/liter; Pipes buffer, 3 mmol/liter; ammonium chloride, 28 mmol/liter;  $\text{NaH}_2\text{PO}_4$ , 4.35 mmol/liter; ferric nitrilotriacetic acid; 0.1 mmol/liter; and sodium selenate, 0.001 mmol/liter. Vitamins and minerals were provided from stock solutions as described (17). Agitation was maintained at 50 rpm to minimize mechanical shear forces, and pH was continuously monitored and maintained at 7.0 by using 2 M HCl.  $\text{O}_2$  served as the sole terminal electron acceptor and was delivered to reactors as compressed air at a constant delivery rate of 4 liters $\cdot$ min $^{-1}$ . Dissolved  $\text{O}_2$  tension (DOT) was monitored by using a polarographic  $\text{O}_2$  probe and meter and was maintained at desired values by using a control loop and switching valves that automatically adjusted the air- $\text{N}_2$  ratio of the influent gas stream. When DOT was maintained at 20% of air saturation, lactate served as the growth-limiting nutrient, and the optical density of steady-state cultures was maintained at 0.68 at 600 nm. Chemostat cultures were also operated with  $\text{O}_2$  as the growth-limiting nutrient. To obtain  $\text{O}_2$  limitation, the air- $\text{N}_2$  ratio of the influent gas stream was manually decreased to 25:50 while the gas addition rate was maintained at 4 liters $\cdot$ min $^{-1}$ . Under these operating conditions, the optical density of the culture was maintained at  $\approx 0.3$  at 600 nm, DOT was below detection of the polarographic  $\text{O}_2$  electrode, and residual concentrations of lactate, pyruvate, and acetate were detected in the spent culture. Collectively, these data measurements confirmed that the reactor was operating with  $\text{O}_2$  limitation.

For selected experiments that required cells that were poised for nanowire production but delayed the display of these structures, chemostat cultures were operated as described above, with the exception that DOT was maintained at 2% of air saturation. When transferred from bioreactors to sealed batch reactors containing HFO as the sole terminal electron acceptor, cells produced nanowires that directly interacted with and transformed iron solids.

*Synechocystis* sp. strain PCC 6803 was cultivated in the chemically defined medium BG11 (18) in a 14-liter continuous-flow BioFlo 3000 (New Brunswick Scientific) reactor with a 9-liter working volume. Light served as the sole energy source and was continuously provided at an average irradiance of 50 microeinsteins $\cdot$ m $^{-2}$  $\cdot$ sec $^{-1}$  by a series of incandescent bulbs that were positioned around the exterior of the reactor. Carbon dioxide served as the sole source of carbon and was provided as a component of compressed air that was delivered to the reactor at 7 liters $\cdot$ min $^{-1}$ . Continuous cultures operated with a dilution rate of  $0.008 \cdot \text{h}^{-1}$  maintained an optical density of  $\approx 0.45$  at 760 nm. Culture density could be increased by increasing average irradiance, confirming that cultures operating under these conditions were light-limited. The concentration of chlorophyll and phycobilin was estimated by monitoring optical density at 678 and 625 nm, respectively. Light-limited cultures were bluish-green in color, and the ratio of absorbance values (678:625 nm)

was maintained at 0.99. To induce a condition of  $\text{CO}_2$  limitation, air entering the reactor was diluted with  $\text{N}_2$  to effectively reduce the  $\text{CO}_2$  concentration of the influent gas from  $\approx 400$  to 100 ppm. This change in gas composition decreased the standing biomass concentration, as measured by optical density at 730 nm, from 0.45 to  $\approx 0.325$ . A color change from bluish-green to yellow corresponded with a significant increase in the chlorophyll-to-phycobilin ratio (1.03 at 678:625 nm), which is consistent with a decrease in phycobilin production (19). Coincidentally, cells produced extracellular appendages that linked cells into flocculated aggregates. These structures were later examined for electrical conductivity.

Syntrophic cocultures of *P. thermopropionicum* with *M. thermoautotrophicus* were cultivated without agitation at 55°C in sealed bottles containing an anaerobic medium with 17 mM propionate as the carbon and energy source as described (12).

**Scanning and Transmission EM.** Samples for SEM were removed from chemostat or sealed batch cultures and immediately fixed by using an anaerobic solution of glutaraldehyde (2% final concentration). Samples were carefully applied to membrane filters with a 0.2- $\mu\text{m}$  pore size and gently washed with pH 7 PBS, dilute PBS (50:50 with deionized water), and then deionized water. Samples were then subjected to a serial dehydration protocol using increasing concentrations of ethanol. After three final changes in 100% ethanol, samples were subjected to critical-point drying by using a CPED2 (Pelco, Redding, CA). Desiccated samples were coated with evaporated carbon and viewed by using a Zeiss-LEO 982 FE-SEM.

**STM and Tunneling Spectroscopy.** Samples from cultures of MR-1 grown with  $\text{O}_2$  limitation and those of *Synechocystis* PCC6803 cultivated with  $\text{CO}_2$  limitation were applied to a freshly cleaved surface of highly ordered pyrolytic graphite (an STM standard flat conducting substrate) and thoroughly washed with an anaerobic solution of PBS followed by anaerobic deionized water to remove salts. The dried samples were examined by using a Molecular Imaging (Tempe, AZ) PicoScan scanning tunneling microscope. STM was performed under ambient conditions in air by using electrochemically sharpened Pt-Ir tips. Topographs were collected under constant-current imaging conditions. Samples were distinguished from linear features inherent to the graphite substrate by choosing imaging condition extremes (e.g., very low-bias voltage, high-setpoint current) that facilitated moving the samples across the graphite surface with the tip. The signatures of the current-voltage and current-distance curves were examined to ensure true tunneling contact over the positions of the samples and over the graphite substrate.

**Fluorescence Microscopy.** Samples for fluorescent microscopy were fixed with an anaerobic solution of glutaraldehyde (2% final concentration) and stained with NanoOrange (Invitrogen) reagent, which fluoresces when bound to amino acids and proteins. Images of stained nanowires and cells were obtained by using a Nikon epifluorescent microscope fitted with a  $\times 100$  oil-immersion objective.

**Mutagenesis.** GSPD, a mutant with a transposon insertion in SOO166 (*gspD*) was isolated by using pMiniHimar RB-1 as described (20). Mutants deficient in Fe(III) reduction were identified as described (21), and phenotypic analysis of the mutants was performed as reported (22). To identify the sites of transposon insertion, total DNA was isolated from the mutants, digested with either BamHI or SphI, ligated, and then used to transform *Escherichia coli* EC100D+ (EPICENTRE Biotechnologies, Madison, WI). Transformed cells were plated on LB/ $K_m$  agar. Purified plasmids were sequenced by using the primer complementary to the 3' end of *HimarI*.

In-frame deletion mutagenesis was performed by using the method originally described by Link *et al.* (23), with minor modifications. Upstream and downstream fragments flanking the *omcA-mtrC* locus were PCR amplified by using *S. oneidensis* MR-1 genomic DNA and primer pairs 5-O/5-I and 3-O/3-I, respectively. The resulting amplicons were fused by overlap extension PCR (24) using complementary 21-bp sequences present on the 5' ends of 5-I and 3-I primers. The fusion PCR amplicon was gel purified and treated with *Taq*DNA polymerase (Qiagen, Valencia, CA) to add a single A overhang and ligated into XcmI-digested pDS3.1 (25). The ligated product was transformed into *E. coli* EC100D pir-116 (EPICENTRE Biotechnologies) and plated on LB with gentamycin selection (15  $\mu$ g/ml). The resulting recombinant plasmids were purified and used to transform *E. coli*  $\beta$ -2155 (26) or WM3064 (27). Plasmids were transferred from *E. coli*  $\beta$ -2155 mating strain to *S. oneidensis* MR-1 by conjugation, and primary integrants were selected by plating on LB medium containing 7.5  $\mu$ g/ml gentamycin. Selection for a second homologous recombination to remove the plasmid sequence was accomplished by growing the primary integrant for 16–18 h in LB-NaCl cultures, followed by sucrose counterselection (28). Colonies growing in the presence of sucrose were screened for sensitivity to gentamycin (7.5  $\mu$ g/ml) and then screened for deletion of the gene of interest by using PCR with the FO/RO primer set. The resulting PCR amplicon was then used as the template for DNA sequencing of the deleted and flanking regions involved in the recombination events (ACGT, Wheeling, IL). Deletion mutagenesis was specific and did not impact phenotypic expression of downstream genes related to metal reduction. Translation of periplasmic mutliheme cytochrome MtrA and the integral outer-membrane protein MtrB were confirmed by Western blots using peptide-specific antibodies.

**Ferrihydrite-Reduction Assays.** Wild-type MR-1, GSPD, and  $\Delta$ MTRC/OMCA were grown in chemostat cultures using a chemically defined medium containing 18 mM lactate as the growth-limiting nutrient and O<sub>2</sub> at a dissolved concentration of  $\approx$ 2% of air saturation. Samples taken at steady state were used to inoculate anaerobic defined medium containing 20 mM silica-substituted ferrihydrite (29) as the sole terminal electron acceptor and 20 mM lactate as the electron donor. Cultures were incubated at 30°C and 25 rpm and sampled for Fe(II) by adding 0.5 ml to 0.5 ml of 1 M HCl with a needle and 1-ml syringe in an anaerobic glovebag. Fe(II) was measured the next day by the ferrozine method (30).

**MFC Assays.** MFCs consisted of anode and cathode compartments, which were cylindrical Pyrex chambers (30 ml of working volume) separated by a proton-exchange membrane (Nafion 424; DuPont). Graphite felt (diameter, 30 mm; thickness, 6 mm; GF series; Electrosynthesis, Amherst, NY) served as both anode and cathode electrodes. Platinum wire contacts (0.5  $\times$  70 mm) were bonded to the electrodes with a conducting epoxy resin (EPOX-4; Electrosynthesis). The cathode electrode was spray-coated with platinum powder at the ratio of 0.4 mg/cm<sup>2</sup> according to the method described in ref. 31. Both compartments of the fuel cell were partially filled with 50 mM phosphate buffer (pH 7.0) containing 0.1 M NaCl. The anode and cathode compartments were continuously purged with N<sub>2</sub> and air to maintain anaerobic and aerobic conditions, respectively.

MR-1 cultures for MFC assays were grown anaerobically in phosphate-buffered basal medium (pH 7.0) containing 30 mM lactate as the electron donor and 60 mM fumarate as the electron acceptor. After 24 h, the cells were harvested and washed twice with 50 mM phosphate buffer (pH 7.0) containing 0.1 M NaCl. The cells were suspended in the same buffer to the final OD<sub>600</sub> of 24. A 0.5-ml aliquot of cell suspension was inoculated into the anode compartment. Lactate was added to the anode compartment as an electron donor to a final concentration of 1.5 mM. The assembled MFCs were placed in an incubator (25°C), and the anode and cathode were connected through a resistance of 10  $\Omega$ . The potential between anode and cathode was measured by using a multimeter (Model 2700; Keithley) linked to a differential multiplexer (Model 7701; Keithley). Data were digitally recorded every 5 min on a personal computer using an interface card (Model PCI-488; Keithley).

This work was supported by the Genomics:Genomes to Life (GTL) and the Natural and Accelerated Bioremediation Research (NABIR) programs of the U.S. Department of Energy (DOE) Office of Biological and Environmental Research (OBER). A portion of the research was performed as part of an Environmental Molecular Sciences Laboratory (EMSL) Scientific Grand Challenge project at the W. R. Wiley EMSL, a national scientific user facility sponsored by OBER and located at Pacific Northwest National Laboratory (PNNL). PNNL is operated for the DOE by Battelle Memorial Institute under Contract DE-AC05-76RL01830. A portion of the research was also performed as part of National Research Laboratory Program (M1-0104-00-0024) and International Collaboration Program (M6-0302-00-0024) sponsored by the Ministry of Science and Technology of Korea and Korea Institute of Science and Technology.

- Nealson, K. H. & Saffarini, D. (1994) *Annu. Rev. Microbiol.* **48**, 311–343.
- Nealson, K. H., Belz, A. & McKee, B. (2002) *Antonie Leeuwenhoek Int. J. Gen. Mol. Microbiol.* **81**, 215–222.
- Lovley, D. R., Coates, J. D., Blunt-Harris, E. L., Phillips, E. J. P. & Woodward, J. C. (1996) *Nature* **382**, 445–448.
- Newman, D. K. & Kolter, R. (2000) *Nature* **405**, 94–97.
- Leang, C., Coppi, M. V. & Lovley, D. R. (2003) *J. Bacteriol.* **185**, 2096–2103.
- Richardson, D. J. (2000) *Microbiology* **146**, 551–571.
- Reguera, G., McCarthy, K. D., Mehta, T., Nicoll, J. S., Tuominen, M. T. & Lovley, D. R. (2005) *Nature* **435**, 1098.
- Beliaev, A. S., Saffarini, D. A., McLaughlin, J. L. & Hunnicutt, D. (2001) *Mol. Microbiol.* **39**, 722–730.
- Myers, C. R. & Myers, J. M. (2003) *Lett. Appl. Microbiol.* **37**, 254–258.
- DiChristina, T. J., Moore, C. M. & Haller, C. A. (2002) *J. Bacteriol.* **184**, 142–151.
- Kim, H. J., Park, H. S., Hyun, M. S., Chang, I. S., Kim, M. & Kim, B. H. (2002) *Enzyme Microb. Technol.* **30**, 145–152.
- Ishii, S., Kosaka, T., Hori, K., Hotta, Y. & Watanabe, K. (2006) *Appl. Environ. Microbiol.* **71**, 7838–7845.
- Lindsay, S. M. (1993) in *Scanning Tunneling Microscopy and Spectroscopy: Theory, Techniques, and Applications*, ed. Bonnell, D. A. (VCH, New York), pp. 335–408.
- Durand, E., Bernadac, A., Ball, G., Lazdunski, A., Sturgis, J. N. & Filloux, A. (2003) *J. Bacteriol.* **185**, 2749–2758.
- Shi, L., Chen, B., Wang, Z., Elias, D. A., Mayer, M. U., Gorby, Y. A., Ni, S., Lower, B. H., Kennedy, D. W., Wunschel, D. S., *et al.* (2006) *J. Bacteriol.* **188**, 4705–4714.
- Myers, J. M. & Myers, C. R. (2003) *Lett. Appl. Microbiol.* **37**, 21–25.
- Kieft, T. L., Fredrickson, J. K., Onstott, T. C., Gorby, Y. A., Kostandarites, H. M., Bailey, T. J., Kennedy, D. W., Li, S. W., Plymale, A. E., Spadoni, C. M. & Gray, M. S. (1999) *Appl. Environ. Microbiol.* **65**, 1214–1221.
- Allen, M. M. (1968) *J. Physiol.* **4**, 1–4.
- McConnell, M. D., Koop, R., Vasil'ev, S. & Bruce, D. (2002) *Plant Physiol.* **130**, 1201–1212.
- Bouhenni, R., Gehrke, A. & Saffarini, D. A. (2005) *Appl. Environ. Microbiol.* **71**, 4935–4937.
- Beliaev, A. S. & Saffarini, D. A. (1998) *J. Bacteriol.* **180**, 6292–6297.
- Saffarini, D. A., Schultz, R. & Beliaev, A. (2003) *J. Bacteriol.* **185**, 3668–3671.
- Link, A. J., Phillips, D. & Church, G. M. (1997) *J. Bacteriol.* **179**, 6228–6237.
- Ho, S. N., Hunt, H. D., Horton, R. M., Pullen, J. K. & Pease, L. R. (1989) *Gene* **77**, 51–59.
- Wan, X.-F., VerBerkmoes, N. C., McCue, L. A., Stanek, D., Connelly, H., Hauser, L. J., Wu, L., Liu, X., Yan, T., Leapart, A., *et al.* (2004) *J. Bacteriol.* **186**, 8385–8400.
- Dehio, C. & Meyer, M. (1997) *J. Bacteriol.* **179**, 538–540.
- Saltikov, C. W., Cifuentes, A., Venkateswaran, K. & Newman, D. K. (2003) *Appl. Environ. Microbiol.* **69**, 2800–2809.
- Blomfield, I. C., Vaughn, V., Rest, R. F. & Eisenstein, B. I. (1991) *Mol. Microbiol.* **5**, 1447–1457.
- Kukkadapu, R. K., Zachara, J. M., Fredrickson, J. K., & Kennedy, D. W. (2004) *Geochim. Cosmochim. Acta* **68**, 2799–2814.
- Stookey, L. L. (1970) *Anal. Chem.* **42**, 779–781.
- Pham, T. H., Jang, J. K., Chang, I. S. & Kim, B. H. (2004) *J. Microbiol. Biotechnol.* **14**, 324–329.